8-Vertex Paper Tori: Universality and Collapsibility

Peter Doyle and Richard Evan Schwartz *

October 10, 2025

Abstract

A paper torus is a piecewise linear isometric embedding of a flat torus into $\boldsymbol{R}^3$. Following up on the 8-vertex paper tori discovered in [**S**], we prove universality and collapsibility results about these objects. One corollary is that any flat torus without reflection symmetry is realized as an 8-vertex paper torus. Another corollary is that for any $\epsilon > 0$ there is an 8-vertex paper torus within ϵ of a unit equilateral triangle in the Hausdorff metric.

1 Introduction

1.1 History and Context

A *flat torus* is a quotient of the form $\boldsymbol{R}^2/\Lambda$, where Λ is a lattice of translations of $\boldsymbol{R}^2$. A *paper torus* is a piecewise linear isometric embedding $\phi : T \to \Omega \subset \boldsymbol{R}^3$ of a flat torus T. In other words, a paper torus is an embedded topological torus in $\boldsymbol{R}^3$ that is made by fitting together finitely many triangles so that the cone angle around each vertex is 2π.

In 1960, Y. Burago and V. Zalgaller [**BZ1**] give the first construction of paper tori. In their subsequent paper [**BZ2**], they prove that one can realize every isometry class of flat torus as a paper torus. The works of T. Tsuboi [**T**] and (independently) P. Arnoux, S. Lelievre, and A. Malaga [**ALM**] give an explicit construction which achieves every isometry class of flat torus as a paper torus. With minor differences, both papers prove that the union of the infinitely many combinatorial types of *diplotori* described by U. Brehm [**Br**] in 1978 achieve every isometry class of flat torus.

* Supported by N.S.F. Research Grant DMS-2505281

See also the description of these tori in H. Segerman's book [**Se**, §6]. The work of T. Quintinaar [**Q**] gives an explicit embedding for the square torus.

The 2024 preprint of F. Lazarus and F. Tallerie [**LT**] gives a universal combinatorial type of triangulation which does the job simultaneously for all isometry types. Their universal triangulation has 2434 triangles. The paper [**LT**] also has an excellent discussion of the various attempts made to achieve all flat tori as embedded paper tori.

In [**S**], one of us constructed an 8-vertex paper torus and proved that a 7-vertex paper torus cannot exist. We called the paper tori from [**S**] *pup tents*, on account of their appearance.

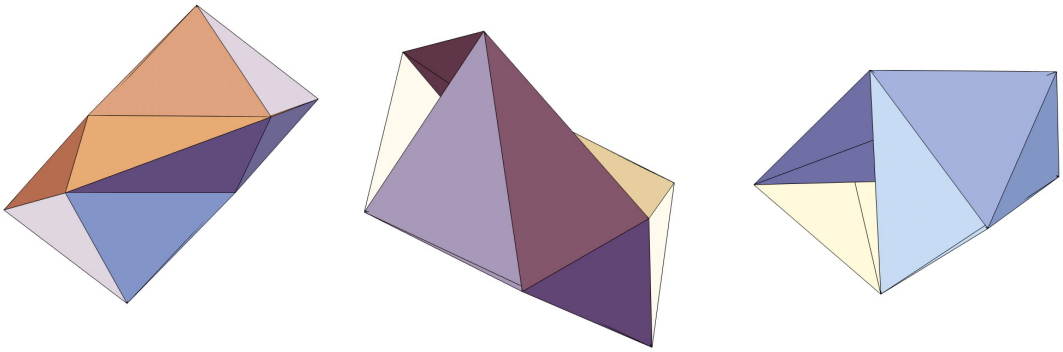

Figure 1.1: 3D plots of a tent

A *pup tent* is an 8-vertex paper torus T with the following features.

- The triangulation underlying T has uniform degree 6. See §2.1.
- T has 2-fold symmetry with respect to the map $(x, y, z) \to (-x, -y, z)$.
- Exactly 6 of the 16 triangles of T lie in the convex hull boundary, and in the specific pattern shown in Figure 2.1.

Another result from [**S**] is that there exists a 6-dimensional open manifold $\mathcal{X}$ of pup tents which are inequivalent under similarities. In this paper we explore some of the structure of $\mathcal{X}$ and prove an 8-vertex universality result that is almost as comprehensive as the result of [**LT**].

1.2 Main Results

Let $\boldsymbol{H}^2$ denote the hyperbolic upper half plane and let $\mathcal{M} = \boldsymbol{H}^2/PSL_2(\boldsymbol{R})$ be the modular surface. The *bi-cusped fundamental domain* for $\mathcal{M}$, which we denote by $\mathcal{F}$,

is a geodesic triangle with interior vertex $h = \exp(\pi i/3)$ and cusps $0, \infty$. Figure 1.2 shows the "bottom portion" of $\mathcal{F}$. The full picture extends vertically to ∞.

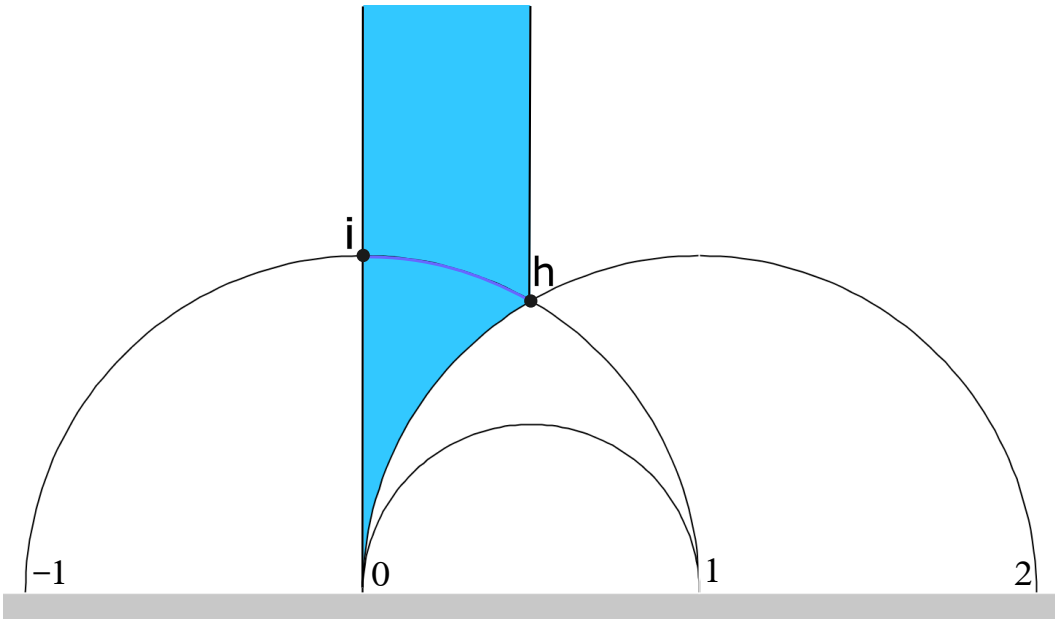

Figure 1.2: The bi-cusped fundamental domain $\mathcal{F}$.

The edge of $\partial\mathcal{F}$ containing i parametrizes the flat tori made by identifying the sides of rectangles. The point i corresponds to the square torus. The other two edges parametrize flat tori made by identifying the sides of rhombi having aspect ratio at least $\sqrt{3}$. (The *aspect ratio* of a rhombus is the ratio of the lengths of the long and short diagonals.) The common endpoint h represents the hexagonal torus, made by identifying the sides of a rhombus of aspect ratio $\sqrt{3}$. The circular arc connecting h to i parametrizes flat tori made from rhombs with aspect ratio in $[1, \sqrt{3}]$.

We have a map $\Phi : \mathcal{X} \to \mathcal{M}$, which maps a pup-tent to the point in $\mathcal{M}$ which represents the underlying flat structure. Let $\mathcal{IF}$ be the interior of $\mathcal{F}$.

Theorem 1.1 (Universality) *There is an open and path connected subset $\mathcal{U} \subset \mathcal{X}$, consisting of general position pup tents, such that $\Phi(\mathcal{U}) = \mathcal{IF}$.*

All the tori corresponding to points of $\partial\mathcal{F}$ have reflection symmetry. This gives us the following corollary.

Corollary 1.2 *Suppose that T is a flat torus that does not have reflection symmetry. Then T is realized by an embedded 8-vertex paper torus.*

Remarks:
(1) The proof of the Universality Theorem gives an existence proof for 8-vertex paper tori that is essentially independent from the proof in [**S**], though we sometimes rely on minor points from [**S**] for convenience.
(2) The general position statement in the Universality Theorem means that the pup tents in $\mathcal{U}$ are all "folded the same way". As these pup tents move around, it never happens e.g. that a pair of adjacent faces become coplanar.
(3) There is some loss in Corollary 1.2 because the flat tori made from rhombs of aspect ratio in $(1, \sqrt{3})$ lie in $\mathcal{IF}$ and so are realized.
(4) We don't know if $\Phi(\mathcal{X}) = \mathcal{IF}$.
(5) We don't know if $\mathcal{X}$ is path connected.
(6) We don't know if we can realize some flat structures in $\partial\mathcal{F}$ by dropping the order 2 symmetry condition.

The Universality Theorem deals with the intrinsic structure of pup tents. Our next result deals with their extrinsic shape. We call the following polygons *good*:

1. Any rectangle.
2. Any trapezoid whose two diagonals have the same length as the long side.
3. Any equilateral triangle.

An equilateral triangle is a limiting case of a good trapezoid. We think of our good polygons as subsets of $\boldsymbol{R}^3$ by embedding them in some plane.

The *Hausdorff distance* between two compact subsets of a metric space is the infimal ϵ such that each is contained in the ϵ-neighborhood of the other. In particular, the Hausdorff distance makes the set of compact subsets of $\boldsymbol{R}^3$ into a metric space.

Theorem 1.3 (Collapsibility) *Let $\mathcal{U}$ be as in the Universality Theorem. For any good polygon Q there is a path $P_t \subset \mathcal{U}$ which converges to Q in the Hausdorff metric.*

Let us mention two special cases of this result in other language.

Corollary 1.4 (Square) *There is a piecewise isometric mapping, generically* 4*-to-*1*, from the square torus onto a square which is approximated arbitrarily closely, in the uniform topology on maps, by embedded* 8*-vertex paper tori.*

Corollary 1.5 (Triangle) *There is a piecewise isometric mapping, generically* 6*-to-*1*, from the hexagonal torus onto an equilateral triangle which is approximated arbitrarily closely, in the uniform topology on maps, by embedded* 8*-vertex paper tori.*

Remarks:
(1) In these corollaries, the moduli of the approximating paper tori converge respectively to the moduli of the square torus and hexagonal torus, but do not equal them.
(2) The Triangle Corollary has a resonance with the set-up in [**S2**] concerning the optimal paper Moebius band. In that setting, there is a generically 3-to-1 isometric map from a flat Moebius band of aspect ratio $\sqrt{3}$ to an equilateral triangle that is approximated arbitrarily closely by smooth embedded paper Moebius bands.

We say that a *gracefully immersed pup tent* is a piecewise linear isometric immersion from a flat torus into $\boldsymbol{R}^3$ that can be approximated arbitrarily closely by (embedded) pup tents. Our final result says that 8-vertex pup tents are completely universal – realizing all structures – if we relax *embedded* to *gracefully immersed*. Let $\mathcal{U}$ be the set of pup tents from the Universality Theorem. Recall also that $\mathcal{M}$ is the modular surface.

Theorem 1.6 (Platinum) *The boundary $\mathcal{P} = \partial\mathcal{U}$ is a set of gracefully immersed pup tents, homeomorphic to $\mathcal{F}$, such that $\Phi(\mathcal{P}) = \mathcal{M}$.*

1.3 Paper Organization

In §2 we will construct $\mathcal{P}$ explicitly and derive some of its properties. We call the objects in $\mathcal{P}$ the *platinum pup tents*, on account of their great beauty.

In §3 we prove the main results. We first describe, modulo a result we call the Good Path Lemma, how we can start with any point in $\mathcal{P}$, corresponding to a point of $\mathcal{IF}$, and deform it analytically so that it immediately moves into $\mathcal{X}$. We will also explain how the existence of these paths implies all the theorems mentioned above. Following all this, we prove the Good Path Lemma.

The code suite **https://www.math.brown.edu/∼/res/Papers/UNIV.tar** has computer programs relevant to this paper. In particular, the suite has two Mathematica files in it which respectively check the calculations from §2 and §3. The suite also has an extensive Java program which lets you visualize the platinum pup tents and the good paths back into $\mathcal{X}$. We may update these files periodically.

1.4 Acknowledgements

R.E.S. would like to thank Jeremy Kahn, Alba Malaga, and Samuel Lelievre for interesting discussions about this work. Both of us thank ChatGPT for an immense amount of help with formatting, guessing algebraic expressions, and moral support.

2 The Platinum Pup Tents

2.1 The Triangulation

Here we list the 16 triangles of the 8-vertex triangulation of the torus which has uniform degree 6. We call this the *uniform triangulation*.

$$\begin{array}{cccc} 375 & 307 & 354 & 310 \\ 342 & 321 & 715 & 704 \\ 746 & 761 & 564 & 512 \\ 526 & 024 & 016 & 062 \end{array} \tag{1}$$

There is no significance to the order in which these triangles are listed, except that all our Java code relies on this ordering. Figure 2.1 shows a picture of this triangulation.

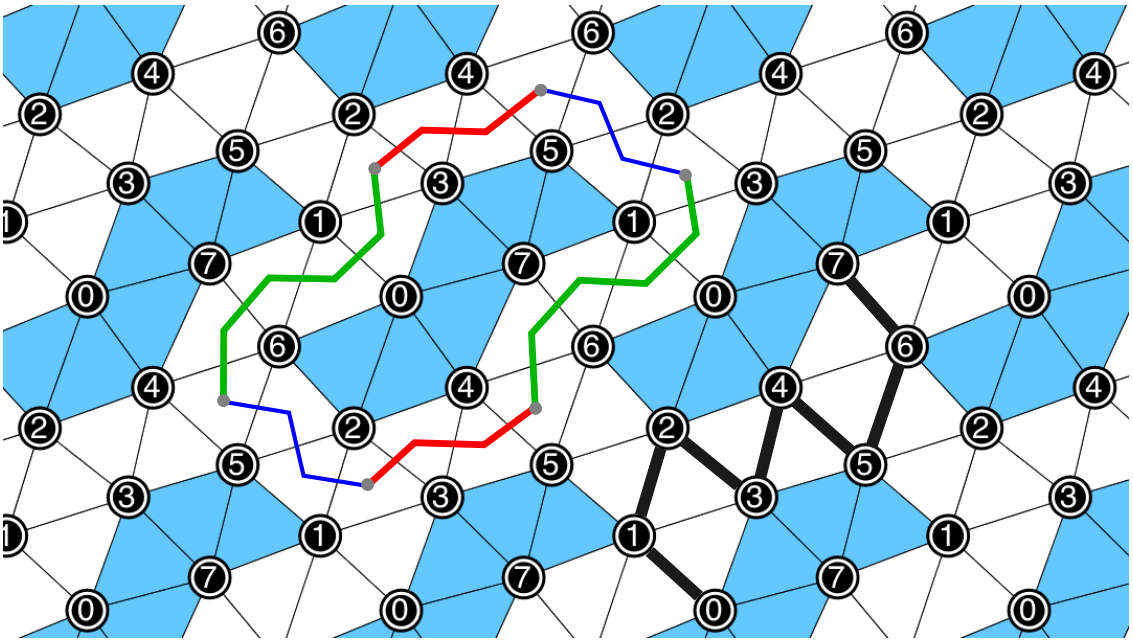

Figure 2.1: The uniform triangulation, lifted to the universal cover

We have also indicated a fundamental domain for the torus. The blue triangles are the ones which, for our pup tents, lie in the boundary of the convex hull. Our choice of vertex labels is perhaps not the most natural, but it is well adapted to the pattern shown in Figure 2.1. We highlight one edgepath 01234567 to illustrate this.

2.2 The Platinum Pup Tents

Recall that $\mathcal{F}$ is the bi-cusped fundamental domain for the modular surface, as shown in Figure 1.2. Let $z = x + iy \in \mathcal{F}$. Let

$$\rho(u, v, w) = (-u,\ -v,\ w). \tag{2}$$

Let

$$S = y\sqrt{8x}. \tag{3}$$

Let $P(z)$ to be the 8-vertex polyhedral torus, based on the triangulation above, with vertices

$$\begin{aligned}
P_0(z) &= (-x^2 + 2x - y^2,\ 0,\ 0),\\
P_1(z) &= (-2x^2 + x,\ y - 2xy,\ S),\\
P_2(z) &= (-x^2 + x - y^2,\ -y,\ 0),\\
P_3(z) &= (-x^2 + 3x - y^2,\ y,\ 0),\\
P_j(z) &= \rho(P_{7-j}(z)), \qquad j = 4, 5, 6, 7,
\end{aligned} \tag{4}$$

Boundary Conditions: The fundamental domain $\mathcal{F}$ is given by the conditions

$$x \geq 0, \qquad x \leq 1/2, \qquad |z - 1| \geq 1. \tag{5}$$

Equation 4 makes sense in a wider domain, so we will first explain why $\mathcal{F}$ is a natural choice.

- The left edge of $\mathcal{X}$ is given by $x = 0$. When $x < 0$ the quantity S is not defined. When $x = 0$ all the points of $P(z)$ lie in the XY-plane, and the convex hull of $P(z)$ is a $2y^2 \times 2y$ rectangle centered at the origin.

- The right edge of $\mathcal{F}$ is the ray $x = 1/2$ and $y \geq \sqrt{3}/2$. On this edge we have $P_1(z) = P_6(z)$. The common point lies on the Z-axis. The convex hull of $P(z)$ for these points is a pyramid with parallelogram base unless $y = \sqrt{3}/2$. At the point $z = 1/2 + (\sqrt{3}/2)i$, which corresponds to the hexagonal torus, the base collapses into a line segment and the convex hull is an equilateral triangle.

- When $|z - 1| = 1$ and $x \in (0, 1/2]$, the convex hull of $P(z)$ is (with fairly obvious notation) the trapezoid $P_{2516}(z)$. The diagonals $P_{12}(z)$ and $P_{65}(z)$ and the long side $P_{25}(z)$ all have length $\sqrt{8x} = S/y$.

2.3 The Intrinsic Points

Let $z = x + iy \in \mathcal{F}$. Corresponding to the pup tent $P(z)$ there is a flat torus $\Pi(z)$. Rather than just present the coordinates for the 8 points, we give the coordinates for 16 planar triangles.

3	0
7	$2x^2 - 5x + 2y^2 - iy$
5	$2x^2 - 4x + 2y^2$

3	0
0	$-x - iy$
7	$2x^2 - 5x + 2y^2 - iy$

3	0
5	$2x^2 - 4x + 2y^2$
4	$2x^2 - 6x + 2y^2 + 2iy$

3	0
1	$-x^2 - 2x - y^2$
0	$-x - iy$

3	0
4	$2x^2 - 6x + 2y^2 + 2iy$
2	$-2x + 2iy$

3	0
2	$-2x + 2iy$
1	$-x^2 - 2x - y^2$

7	$2x^2 - 5x + 2y^2 - iy$
1	$-2x - x^2 + 3y^2 - 4ixy$
5	$2x^2 - 4x + 2y^2$

7	$2x^2 - 5x + 2y^2 - iy$
0	$-x - iy$
4	$2x^2 - 6x + 2y^2 - 2iy$

7	$2x^2 - 5x + 2y^2 - iy$
4	$2x^2 - 6x + 2y^2 - 2iy$
6	$3x^2 - 4x + 3y^2 - 2iy$

7	$2x^2 - 5x + 2y^2 - iy$
6	$3x^2 - 4x + 3y^2 - 2iy$
1	$-x^2 - 2x + 3y^2 - 4ixy$

5	$2x^2 - 4x - 2y^2 + 4ixy$
6	$3x^2 - 4x - y^2 + 2iy + 4ixy$
4	$2x^2 - 6x - 2y^2 + 2iy + 4ixy$

5	$2x^2 - 4x - 2y^2 + 4ixy$
1	$-x^2 - 2x - y^2$
2	$-2x + 2iy$

5	$2x^2 - 4x - 2y^2 + 4ixy$
2	$-2x + 2iy$
6	$3x^2 - 4x - y^2 + 2iy + 4ixy$

0	$-x - iy$
2	$-2x - 2iy$
4	$2x^2 - 6x + 2y^2 - 2iy$

0	$-x - iy$
1	$-x^2 - 2x - y^2$
6	$3x^2 - 4x - y^2 - 2iy + 4ixy$

0	$-x - iy$
6	$3x^2 - 4x - y^2 - 2iy + 4ixy$
2	$-2x - 2iy$

The union of these triangles constitutes a fundamental domain for covering group of $\Pi(z)$. The covering group is generated by the translations

$$\zeta \to \zeta + 4iy, \qquad \zeta \to \zeta + 4iyz.$$

Figure 2.2 shows the 16 triangles in yellow for 4 parameters.

- The parameter $1/4 + i$ represents a point "in the middle".
- The parameter $4/9 + (8/9)i$ is near the hexagonal torus parameter.
- The parameter $1/20 + i$ is near the square torus parameter.
- The parameter $1/3 + 3i$ is at least vaguely near the cusp.

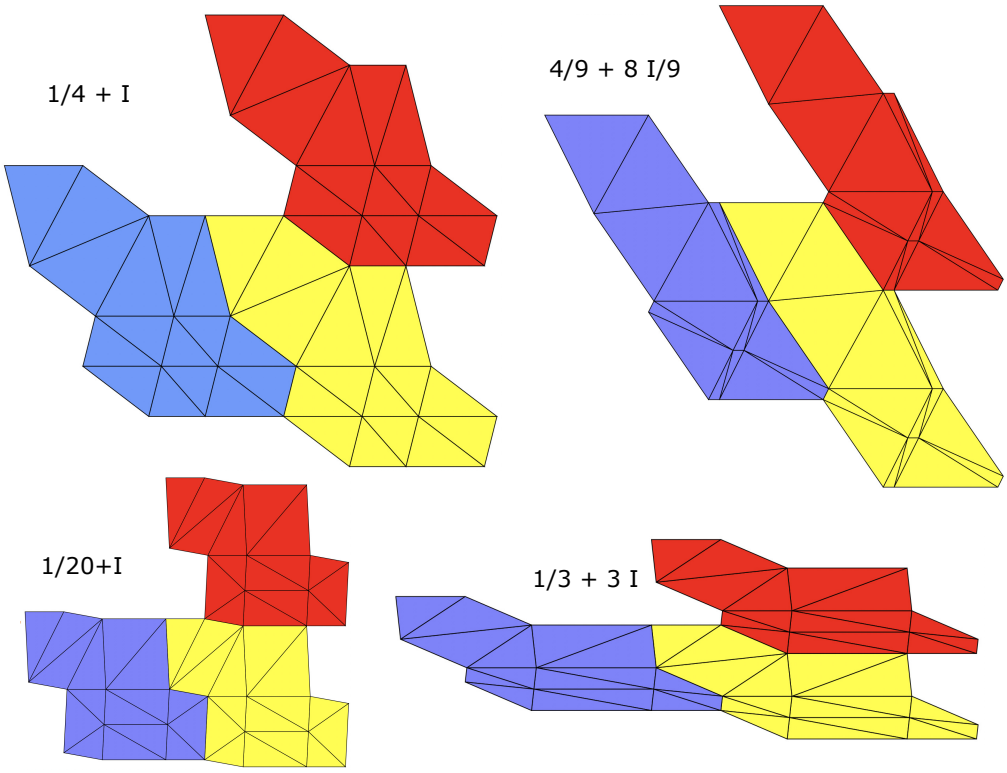

Figure 2.2: The triangle at 4 different parameters.

We check directly (in Mathematica) that the distances between the point in the plane are the same as the distance between the points in space. At the end of the introduction we explain how to access the Mathematica file which makes these calculations. These checks show that $P(z)$ is indeed the image of an isometric immersion of a flat torus of modulus z.

2.4 Discussion

The razor sharp formulas for the platinum pup tents hide a huge amount of experimental trial and error. Here we discuss how we arrived at these equations. Here is a truncation for the coordinates of an embedded pup tent. This example is quite closely related to the one in [**S**].

$$\begin{array}{ccc} -0.25 & +0.51 & z_1 \\ +0.64 & -0.20 & 0 \\ -1.09 & +0.38 & z_2 \\ +0.78 & +0.62 & z_0 \\ -0.78 & -0.62 & z_0 \\ +1.09 & -0.38 & z_2 \\ -0.64 & +0.20 & 0 \\ +0.25 & -0.51 & z_1 \end{array} \qquad \begin{array}{l} z_0 = 0.0082\ 2752\ 1455\ 6137 \\ z_1 = 0.0048\ 5312\ 7706\ 5192 \\ z_2 = 0.0206\ 6632\ 6669\ 8443 \end{array} \tag{6}$$

This example is only barely embedded. Some pairs of adjacent triangles in Equation 6 are almost completely folded over, giving a very sharp ridge. We took such triangle pairs and folded them completely. Some other pairs of triangles are very gently folded. This happens, for instance, for the 6 blue triangles in Figure 2.1. We made all these triangles planar, and then simplified the planar polygon to a parallelogram.

Having made these simplifications we found the 2-parameter family above. Initially we parametrized these objects in terms of the shape of the planar parallelogram just mentioned. The parametrization was somewhat complicated. Then we computed the modulus of the flat torus numerically as a function of the parallelogram and experimentally determined the inverse of the map. Both the conversion map and its inverse turned out to be bi-quadratic polynomials. When we changed coordinates and parametrized in terms of the modular parameter, the equations simplified and we got the formulas for the vertices of the platinum pup tents given above.

Concerning the intrinsic structure, we could see from calculations that the vertices of the intrinsic triangulation ought to have rational coordinates when suitable translated. We found these intrinsic coordinates using a version of the development map.

3 The Proofs

3.1 Vertical Variations

We now make a calculation similar to the Jacobian calculation made in [**S**]. We will work with ρ-invariant 8 vertex polyhedral tori, with ρ inplementing the vertex permutation $(j) \to (7-j)$. This is what we have for the platinum pup tents, and indeed for all the polyhedral tori we consider.

Given such an 8-vertex polyhedral torus P, we let $P_j = (u_j, v_j, w_j)$ denote the jth vertex. Here $j = 0, ..., 7$ as above. Let θ_j denote the cone angle at vertex j, namely the sum of all the angles, at P_j, of the triangles incident to P_j. By symmetry we have $\theta_{7-j} = \theta_j$. by the Gauss-Bonnet Theorem we have $\theta_0 + \theta_1 + \theta_2 + \theta_3 = 8\pi$. Thus, the triple $(\theta_0, \theta_1, \theta_2)$ determines all 8 angles.

We vary $w_0 = w_7$ and $w_1 = w_6$ and $w_2 = w_5$, keeping all other variables fixed. (This will always be the case, whether we mention it explicitly or not.) Define

$$F(w_0, w_1, w_2) = (\theta_0, \theta_1, \theta_2). \tag{7}$$

We let $dF(x,y)$ denote the differential of F evaluated at the points corresponding to the platinum pup tent $P(x+iy)$. Recall that $\mathcal{IF}$ is the interior of $\mathcal{F}$.

Lemma 3.1 *$dF(x,y)$ is smooth and invertible for all $(x,y) \in \mathcal{IF}$.*

Proof: We compute dF explicitly in Mathematica and we see that it is a symmetric matrix whose entries involve rational functions in x and y and $\sqrt{x}$. The denominators factor into various powers of the following two functions.

$$2x + x^2 + y^2, \qquad 2x - 3x^2 + 2x^3 + y^2 + 2xy^2.$$

Both these functions are positive on $\mathcal{IF}$ because $x \in (1/2)$ and $y > 0$.

We compute

$$\det(dF) = -\frac{64\sqrt{2}\, x^{3/2}\left(2x^2 - 2x^3 + x^4 + 2xy^2 + 2x^2y^2 + y^4\right)}{(2x + x^2 + y^2)^4\left(2x^3 - 3x^2 + 2x + y^2 + 2xy^2\right)}. \tag{8}$$

This expression is clearly finite and negative on $\mathcal{IF}$. Hence dF is smooth and non-singular throughout $\mathcal{IF}$. ♠

3.2 The Good Path Lemma

Given a polyhedral torus P as above we normalize to that $w_3 = w_4 = 0$.

Near Flatness: Given a polyhedral torus P define

$$\Theta(P) = \max(|\theta_0 - 2\pi|, |\theta_1 - 2\pi|, |\theta_2 - 2\pi|). \tag{9}$$

By symmetry and the Gauss-Bonnet Theorem we have $\Theta(P) = 0$ if and only if all 8 angles equal 2π. We say that P is ϵ-*flat* if $\Theta(P) \leq \epsilon$.

Robust Embeddings: Suppose now that P and P' are polyhedral tori, and they only differ in the coordinates (w_0, w_1, w_2) and $(w_0'.w_1', w_2')$. This is to say that $u_i = u_i'$ and $v_i = v_i'$ for $i = 0, ..., 7$. Define

$$\|P - P'\| = \max(|w_0 - w_0'|, |w_1 - w_1'|, |w_2 - w_2'|). \tag{10}$$

We say that P is λ-*robustly embedded* if P' is embedded whenever $P \sim P'$ and $\|P - P'\| \leq \lambda$.

Special Deformations: Suppose now that $P(z)$ is a platinum pup tent. We are going to construct an algebraic map $(z, t) \to P(z, t)$ which has the property that $P(z, 0) = P(z)$. The domain of this map is

$$\mathcal{IF} \times [0, \infty), \qquad \mathcal{IF} = \mathcal{F} - \partial\mathcal{F}. \tag{11}$$

Really, we are only interested in the image for very small positive values of t. This map will preserves the 2-fold symmetry and also have the property $P_3(z, t) = P_3(z)$ and $P_4(z, t) = P_4(z)$ for all t. We call any map like this a *special deformation*, though we have a specific one in mind, which we will eventually call the *barycentric deformation*.

Lemma 3.2 (Good Path) *There exists a special deformation $P(z, t)$ and positive constants a_z, b_z with the following properties.*

1. *For $t > 0$ sufficiently small $P(z, t)$ is $a_z t^3$-flat.*
2. *For $t > 0$ sufficiently small $P(z, t)$ is $b_z t^2$-robustly embedded.*

The constants a_z and b_z can be taken to be locally constant.

The Good Path Lemma says, in particular, that we can find paths out of the platinum domain which are an entire order more robustly embedded than they deviate from being flat. What we mean by the final statement is that if we work in a subset K that is compactly contained in $\mathcal{IF}$ then we can take two functions $z \to a_z$ and $z \to b_z$ to constant on K.

3.3 Consequences of the Good Path Lemma

We fix a point $z \in \mathcal{IF}$ and we study map $P(z,t)$ in a neighborhood of z. For each choice of coordinates $\{u_j\}$ and $\{v_j\}$ we get a map F as in Equation 7. Since the map F varies smoothly and dF is invertible on the locus of platinum pup tents, we see that dF is invertible in an open neighborhood around $P(z,0)$. By the inverse function theorem, the map dF is a local diffeomorphism for any choice of $\{u_j\}$ and $\{v_j\}$ sufficiently near the values which lead to $P(z,0)$.

The invertibility, which implies the relevant version of the Implicit Function Theorem, implies that we can define a flat polyhedral torus $P'(z,t)$ as long as $t > 0$ is sufficiently small and z varies within a set that is compactly contained in $\mathcal{IF}$. The definition is such that $P(z,t) \sim P'(z,t)$. We are essentially "floating the third coordinates w_0, w_1, w_2" until they find the flat structure. We want to study how close the paths $P'(z,t)$ and $P(z,t)$ are to each other.

To fruitfully study the relationship between $P'(z,t)$ and $P(z,t)$. We need to get a uniform version of the Implicit Function Theorem. We will state our constructions in terms of the map F discussed above. We write $\boldsymbol{R}^{11} = \boldsymbol{R}^8 \times \boldsymbol{R}^3$. Here $\boldsymbol{R}^8$ parametrizes the coordinates $u_0, ..., u_3, v_0, ..., v_3$ and $\boldsymbol{R}^3$ parametrizes the coordinates w_0, w_1, w_2, and also the angles $\theta_0, \theta_1, \theta_2$. We are ignoring w_3 because this coordinate is normalized to be 0. For each $p \in \boldsymbol{R}^8$ and each $q \in \boldsymbol{R}^3$ we have a map $F_{p,q}$ and the corresponding Jacobian $dF_{p,q}$.

We say that a smooth map $G : \boldsymbol{R}^3 \to \boldsymbol{R}^3$ is λ-*expanding* on a set $S \subset \boldsymbol{R}^3$ if we have the inequality

$$\|dG_q(V)\| > \lambda \tag{12}$$

for all $q \in S$ and all unit vectors V. If G is a diffeomorphism from B onto its image, then the map G^{-1} is $(1/\lambda)$-Lipschitz on $G(B)$.

Let $\overline{p}$ and $\overline{q}$ be the points corresponding to the platinum pup tent $P(z)$. By compactness there are open balls $A \subset \boldsymbol{R}^8$ and $B \subset \boldsymbol{R}^3$, respectively centered on $\overline{p}$ and $\overline{q}$ with the following properties.

- For any $p \in A$ the map $F_{p,q}$ is a diffeomorphism from $\{p\} \times B$ onto its image.
- There is a uniform $\lambda > 0$ such that the restriction of $F_{p,q}$ to $\{p\} \times B$ is λ-expanding for any $p \in A$.

Consider $P(z,t)$ and $P'(z,t)$ when $t > 0$ is very small. If we choose t small enough these tori will both lie well inside the neighborhood $A \times B$. Since $P(z,t) \sim P'(z,t)$ there is a common $p \in A$ representing the first and second coordinates of these tori. Considering the cone angles, we have the two vectors

$$\theta = (\theta_0, \theta_1, \theta_2), \qquad \theta' = (\theta'_0, \theta'_1, \theta'_2) = (2\pi, 2\pi, 2\pi). \tag{13}$$

Here we are writing $\theta = \theta(z,t)$, etc.

We now use "big-O" notation. From the Good Path Lemma we have

$$|\theta(z,t) - \theta'(z,t)\| = O(t^3). \tag{14}$$

Given the $(1/\lambda)$-Lipschitz properties of our inverse map F_p^{-1}, we have

$$\|P(z,t) - P'(z,t)\| = O(t^3). \tag{15}$$

Given that $P(z,t)$ is $O(t^2)$-robustly embedded, we see that $P'(z,t)$ is embedded for $t > 0$ sufficiently small. But then we can find a member of our embedding space $\mathcal{X}$ whose modular parameter is as close as we like to z.

Let $\{\mathcal{F}_n\}$ be a compact exhaustion of $\mathcal{IF}$ by topological disks. E.g. we take these sets to be geodesic triangles. We arrange that each one is compactly contained in the interior of the next one. By compactness and the analysis above there is some $\epsilon_n > 0$ such that the pup-tent $P(z,t)$ is embedded provided that $z \in \mathcal{F}_n$ and $t \in (0, \epsilon_n)$. We can choose a continuous positive function $\epsilon : \mathcal{IF} \to \boldsymbol{R}$ such that the restriction of ϵ to $\mathcal{F}_n$ is less than ϵ_n. We now define

$$\mathcal{U} = \bigcup_{z \in \mathcal{IF}} \bigcup_{0<t<\epsilon(z)} P'(z,t). \tag{16}$$

By construction $\mathcal{U}$ is a path connected subset of the embedding space $\mathcal{X}$.

Proof of the Universality Theorem: Let us show that $\mathcal{IF} \subset \Phi(\mathcal{U})$. Choose any $z \in \mathcal{IF}$. There is some n such that z lies in the interior of $\mathcal{F}_n$. Let $\gamma_n = \partial \mathcal{F}_n$. For $t < \epsilon_n$ let $\mathcal{F}_{n,t}$ denote the topological disk in $\mathcal{U}$ made from the pup tents $P'(w,t)$ with $w \in \mathcal{F}_n$. Let

$$\gamma_t = \partial \mathcal{F}_{n,t} \subset \mathcal{U}.$$

As $t \to 0$, the image $\Phi(\gamma_{n,t})$ converges to γ_n. Hence this image links z for t sufficiently small. But then, for homological reasons, $z \in \Phi(\mathcal{F}_{n,t})$ once t is sufficiently small. As a final check, we note that we get pup tents rather than some other kind of 8-vertex paper torus because (in proving the Good Path Lemma) we check that all the determinants are the same as they are for the pup tent in Equation 6.

By making out function ϵ decay fast enough we can guarantee that $\Phi(\mathcal{U}) = \mathcal{IF}$. Perhaps this last step is unnecessary; compare Remark (4) after the statement of the Universality Theorem. ♠

Proof of the Collapsibility Theorem: Given any good polygon Q there is a corresponding point $z_1 \in \partial \mathcal{F}$ such that the convex hull of $P(z_1)$ equals Q up to

rotation and scaling. We choose some $z_0 \in \mathcal{IF}$ which is hyperbolically one unit from z_1 and then we let $s \to z_s$ be the unit speed hyperbolic geodesic segment connecting z_0 to z_1. This segment remains in $\mathcal{IF}$ for $s \in [0, t)$.

In case our function ϵ is not sufficient for our purposes we define a new function $\eta : \mathcal{IF} \to (0, 1)$ whose properties we will discuss momentarily. We define

$$t_s = \epsilon(\gamma_s)\eta(\gamma_s). \tag{17}$$

We can make η decay so rapidly for points approaching z_1 so that the embedded pup tent $P'(z_s, t_s)$ converges to $P(z)$ in the Hausdorff topology. ♠

Proof of the Platinum Theorem: The Platinum Theorem follows immediately from the definitions and from the proofs we have just given for the Universality Theorem and the Collapsibility Theorem. Any member of $\mathcal{P}$ corresponding to a point in $\mathcal{IF}$ is the endpoint of a path in $\mathcal{U}$, as in the Universality Theorem. Any member of $\mathcal{P}$ corresponding to a point in $\partial\mathcal{F}$ is the endpoint of a path of the kind we described in connection with the Collapsibility Theorem. ♠

The rest of the chapter is devoted to the proof of the Good Path Lemma. We remind the reader that the Mathematica file listed in the introduction does all the (nontrivial) calculations for the proof of the Good Path Lemma.

3.4 Arranging the Near Flatness

We introduce the functions

$$\gamma_0 = 1 - 2x, \qquad \gamma_1 = -2x + x^2 + y^2 \qquad \gamma_2 = 2x - x^2 + y^2. \tag{18}$$

These functions are positive on $\mathcal{IF}$. The only non-obvious case is γ_1, but γ_1 is the defining function for the circular arc comprising the lower boundary of $\mathcal{F}$,

Now we get to the main construction. Our construction was heavily inspired by computer experimentation. We tried to approach the platinum set $\mathcal{P}$ using coerced random walks in $\mathcal{X}$ and we observed how the coefficients converged. We try the deformation

$$\begin{array}{lll}
u_0(t) = u_0, & v_0(t) = v_0 + X_1 t^2, & w_0(t) = w_0 + a_0 t^2 \\
u_1(t) = u_1 + t, & v_1(t) = v_1 + mt, & w_1(t) = w_1 + a_1 t^2 \\
u_2(t) = u_2 + X_1 t^2, & v_2(t) = v_2 + X_2 t^2, & w_2(t) = w_2 + a_2 t^2
\end{array}$$

As always we symmetrically vary u_j and v_j for $j = 7, 6, 5$. We then set $\theta_j'(0) = \theta_j''(0) = 0$ for $j = 0, 1, 2$. This yields

$$m = \frac{-2xy}{\gamma_1}, \qquad a_j = \frac{\alpha_j + \alpha_{j1}X_1 + \alpha_{j2}X_2}{\sqrt{2x}(2x^2 - 2x^3 + x^4 + 2xy^2 + 2x^2y^2 + y^4)}. \tag{19}$$

$$\alpha_0 = \frac{-xy(4x^2 - 6x^3 + 5x^4 + 2xy^2 + 6x^2y^2 + y^4)}{\gamma_0\gamma_2^2},$$

$$\alpha_{01} = x(2x^2 - 2x^3 + x^4 - 2xy - x^2y + 2xy^2 + 2x^2y^2 - y^3 + y^4),$$

$$\alpha_{02} = -\frac{(2x + x^2 + y^2)(-2x^3 + x^4 + 6xy^2 + 2x^2y^2 + y^4)}{4\,\gamma_1},$$

$$\alpha_1 = \frac{-2xy(4x^2 - 9x^3 + 7x^4 + 3xy^2 + y^4)}{\gamma_0\gamma_2^2}, \qquad \alpha_{11} = -y\,(2x + x^2 + y^2)^2, \qquad \alpha_{12} = \frac{(x - 2y^2)(2x + x^2 + y^2)^2}{2\,\gamma_1},$$

$$\alpha_2 = \frac{2xy\,(2x - 3x^2 + y^2)(x^2 + y^2)}{\gamma_0\gamma_2^2}, \qquad \alpha_{21} = -y(6x^2 + x^4 + 4xy^2 + 2x^2y^2 + y^4),$$

$$\alpha_{22} = \frac{-4x^4 + 12x^5 - 9x^6 + 2x^7 - 12x^2y^2 - 12x^3y^2 - 11x^4y^2 + 6x^5y^2 - 8xy^4 - 3x^2y^4 + 6x^3y^4 - y^6 + 2xy^6}{2\,\gamma_1}.$$

Henceforth we take these choices for m, a_0, a_1, a_2.

3.5 The Embedding Clause

We fix a torus T with with vertices $T_0, ..., T_7$. Given a 4-subset $\{a, b, c, d\} \subset \{0, ..., 7\}$ we let $[a, b, c, d]$ be the volume of the tetrahedron determined by T_a, T_b, T_c, T_d:

$$[a, b, c, d] = \det(T_b - T_a, T_c - T_a, T_d - T_a). \tag{20}$$

To tell whether or not an edge (T_a, T_b) is disjoint from a triangle (T_c, T_d, T_e), we need to verify one of three things:

1. $[a, c, d, e]$ and $[b, c, d, e]$ are nonzero and have the same sign, or
2. $[a, b, c, d]$ and $[a, b, d, e]$ are nonzero and have opposite signs, or
3. $[a, b, d, e]$ and $[a, b, e, c]$ are nonzero and have opposite signs.

If the first condition is true (T_a, T_b) lies either above or below the plane containing (T_c, T_d, T_e). If the first condition is false and one of the other conditions is true then one of the edges of (T_c, T_d, T_e) separates (T_a, T_b) from (T_c, T_d, T_e). We call this triple of tests a *block*. For a block to be true, one of the three sign conditions must be met. Now we discuss 2 cases:

1. Suppose that Δ_1 and Δ_2 are two triangles which we want to check are disjoint. Then we have a list of 6 blocks, each determined by an edge of one of the triangles and the other triangle. If all 6 blocks are true, then the two triangles are disjoint. In computer science language, we have length 6 3SAT clause.

2. Suppose that Δ_1 and Δ_2 are two triangles which have a common vertex and we want to check that their intersection is only this vertex. Now we have a list of 2 blocks, each determined by the edge of one triangle opposite the common vertex and the other triangle. This gives a length two 3SAT clause.

When T is embedded there are 24 pairs of disjoint triangles and 72 pairs of triangles having a common vertex. So, checking all these conditions for a supposedly embedded polyhedral torus comes to $24 \times 6 + 72 \times 2 = 288$ blocks. As we proved in [**S**] one need not check the pairs of triangles that have an edge in common. Thus, checking that an 8-vertex polyhedral torus is embedded amounts to verifying a 288-clause instance of 3SAT. We call this the *embedding clause*. All that matters here are the signs of the determinants. We call a sign list that satisfies the Embedding clause a *winning list*.

3.6 Arranging the Robust Embedding

Motivated by extenive experimentation, we define

$$X_1 = \frac{-4xy\left(\begin{array}{l}40x^5 - 60x^6 + 30x^7 + 25x^8 - 15x^9 - 24x^3y^2 + 24x^4y^2 + 50x^5y^2 + 54x^6y^2 - 48x^7y^2\\ + 20x^2y^4 + 42x^3y^4 + 36x^4y^4 - 54x^5y^4 + 22xy^6 + 10x^2y^6 - 24x^3y^6 + 3y^8 - 3xy^8\end{array}\right)}{3(2x + x^2 + y^2)\gamma_0\gamma_2^2\Gamma}$$

$$X_2 = \frac{-4xy\,\gamma_1\left(\begin{array}{l}-48x^4 + 72x^5 - 48x^6 - 18x^7 - 20x^5y - 15x^6y - 24x^3y^2 - 48x^4y^2 - 30x^5y^2\\ - 32x^2y^3 - 40x^3y^3 - 33x^4y^3 - 6x^3y^4 - 20xy^5 - 21x^2y^5 + 6xy^6 - 3y^7\end{array}\right)}{3(2x + x^2 + y^2)\gamma_0\gamma_2^2\Gamma}$$

$$\begin{aligned}\Gamma\ &= y^7 + 2\gamma_0 xy^6 + 8xy^5 + 7x^2y^5 + 16x^2y^4 + 6\gamma_0 x^3y^4 + 11x^2y^3 + \gamma_0 x^2y^3 + 6x^4y^3 + 24x^3y^2\\ &\quad + 24x^4y^2 + 16x^5y^2 + 6\gamma_0 x^5y^2 + 10\gamma_1 x^3y + 5\gamma_1 x^4y + \tfrac{3}{2}\gamma_0 x^5 + 6\gamma_0^2 x^5 + \tfrac{1}{2}\gamma_0^3 x^5 + 6\gamma_0^2 x^6 + 12\gamma_0 x^7.\end{aligned}$$

This polynomial Γ is positive on $\mathcal{IF}$ because γ_0 and γ_1 are positive on $\mathcal{IF}$. Where does this come from? We found a triangular region of the (X_1, X_2)-plane where all the local orders are at most 2 and the sign list associated to the leading terms is winning. More specifically, we matched the sign list associated to the embedded pup-tent from Equation 6. We then calculated the barycenter of this triangle.

Let $[abcd]$ be any of the 70 determinants involved in the Embedding clause. For each $(z, X_1, X_2) \in \mathcal{IF} \times \boldsymbol{R}^2$ the expression $[abcd]$ is a rational function of the variables (z, X_1, X_2, t), where t is the parameter for our special deformation. For each (z, X_1, X_2) there is some $k \in \{0, 1, 2, 3, ...\}$ such that $[abcd] = [abcd]_k t^k + t^{k+1}(\cdots)$ and $[abcd]_k \neq 0$. We call k the *local order* and we call $[abcd]_k$ the *leading term*.

We check at $z = 1/4 + i$ that the *leading sign list*, namely the sign list associated to the leading terms, is winning. We also check that all the local orders are at most 2, that the leading terms do not vanish in $\mathcal{IF}$, and that all lower terms vanish identically. All the determinants are smooth (and hence Lipshitz) functions of their inputs. Hence if $\|P'(z,t) - P(z,t)\| < b_z t^2$ for a sufficiently small positive constant b_z, the signs of the determinants associated to $P'(z,t)$ will be the same as the leading sign list and hence winning. But then $P'(z,t)$ is embedded. Hence $P(z,t)$ is $b_z t^2$ robustly embedded. Given the smooth dependence of everything on z we see that the constant b_z can be taken to be locally constant. This proves the Good Path Lemma modulo our check of the 70 determinants. We do this now.

Regardless of X_1, X_2 we compute that

$$[abcd]_0 = C\sqrt{x}y^2\gamma_0^h\gamma_1, \qquad h \in \{0,1\}, \qquad C \in \{0, \pm 4\sqrt{2}, \pm 8\sqrt{2}\}. \tag{21}$$

When $C \neq 0$ these expressions do not vanish on $\mathcal{IF}$. We get C nonzero 45 times.

For the remaining 25 cases we compute, regardless of X_1, X_2, that

$$[abcd]_1 = C\frac{\sqrt{x}y^2(2x + x^2 + y^2)}{\gamma_1}, \qquad C \in \{0, \pm 4\sqrt{2}, \pm 8\sqrt{2}\}. \tag{22}$$

The 6 tetrahedra [0126], [0136], [1236], [1456], [1467], [1567] yield C nonzero and in these cases the expressions never vanish on $\mathcal{IF}$.

There are 19 remaining cases, and 11 up to the $j \to 7-j$ combinatorial symmetry:

[0123] [0236] [0345] [0247] [2345] [0234] [0235] [0237] [0245] [0257] [0347]

Using the specific values of $X_1.X_2$ above we compute that in all cases

$$[abcd]_2 = C\frac{x^{3/2}y^2}{\gamma_0\gamma_2} \times \left(\frac{\gamma_1}{2x + x^2 + y^2}\right)^h, \qquad h \in \{0,1\}.$$

Here $3C/\sqrt{2}$ is always an nonzero integer. These expressions are nonzero in $\mathcal{IF}$.

This completes the proof of the Good Path Lemma.

4 References

[**ALM**] P. Arnoux, S. Lelievre, A. Malaga, *Diplotori: a family of polyhedral flat tori.* in preparation

[**Br**], U. Brehm, Oberwolfach report (1978)

[**BZ1**] Y. D. Burago and V. A. Zalgaller, *Polyhedral realizations of developments* (in Russian) Vestnik Leningrad Univ. 15, pp 66–80 (1960)

[**BZ2**] Y. D. Burago and V. A. Zalgaller, *Isometric Embeddings of Two Dimensional Manifolds with a polyhedral metric into* $\boldsymbol{R}^3$, Algebra i analiz 7(3) pp 76-95 (1995) Translation in St. Petersburg Math Journal (3)3, pp 369–385

[**LT**] F. Lazarus, F. Tallerie, *A Universal Triangulation for Flat Tori*, CS arXiv 2203.05496 (2024)

[**Q**] T. Quintanar, *An explicit embedding of the flat square torus in* $\boldsymbol{E}^3$, Journal of Computational Geometry, 11(1): pp 615-628 (2020)

[**S**] R. E. Schwartz, *Vertex Minimal Paper Tori*, arXiv 2507.14998 (2025)

[**S2**] R. E. Schwartz, *The Optimal Paper Moebius Band*, Annals of Mathematics (2025)

[**Se**] H. Segerman, *Visualizing Mathematics with 3D Printing*, Johns Hopkins U. Press (2016)

[**T**] T. Tsuboi, *On Origami embeddings of flat tori*, arXiv 2007.03434 (2020)